TOWARDS UNDERSTANDING THE NATURE OF HIGH FREQUENCY BACKSCATTER FROM CELLS AND TISSUES: AN INVESTIGATION OF BACKSCATTER POWER SPECTRA FROM DIFFERENT CONCENTRATIONS OF CELLS OF DIFFERENT SIZES

M.C. Kolios[1,2], G.J. Czarnota[1,3] A. Worthington[3], A. Giles[3], A.S. Tunis[2] and M.D. Sherar[2,3]

[1]Dept. of Mathematics, Physics and Computer Science, Ryerson University, Toronto, ON, M5B2K3, Canada,
[2]Dept. of Medical Biophysics, University of Toronto, 610 University Avenue, Toronto, ON, M5G2M9, Canada
[3]Ontario Cancer Institute, Princess Margaret Hospital, 610 University Avenue, Toronto, ON, M5G2M9, Canada

Abstract – *During cell death a series of structural changes occur within the cell. We have shown that cell ensembles and tissues undergoing structural changes associated with various cell death pathways can be detected using high-frequency ultrasound. In our effort to better understand the nature of backscatter from collections of cells (which emulate tissues), we have collected raw RF backscatter data from cells of two different sizes in solutions for a series of concentrations or in pellet form. Human acute myeloid leukemia cells (AML-5, ~10μm in diameter) and transformed prostate cells (~25-30μm in diameter) were imaged either in suspension or in pellet form. Images and radiofreqeuncy data were acquired using a VS40B ultrasound instrument (VisualSonics Inc., Toronto, Ont) and 20MHz, 30MHz and 40MHz transducers with -6dB bandwidths approaching 100%. The cells were either imaged in degassed phosphate buffered solution in which their volumetric fraction increased from 0.0025% to 2%, or in pellet form by using a swinging bucket centrifuge. It was found that the backscatter power (as measured by the mid-band fit) increased by ~ 3 dB for both cell types in dilute solutions for which the volumetric concentration was doubled for a specific range of cell concentrations (which was dependent on cell size). In pellet form the backscatter power from the prostate cell pellets was ~12-14dB greater than the AML cell pellets. A comparison of the spectral slopes also strongly suggests a change in the scattering source contributions when the cells are in pellets: the spectral slope was negative for all concentrations for prostate cells imaged at 40MHz, but positive when measured in pellets. This is consistent an increased contribution to the backscatter of smaller sized scatterers (such as the cell nucleus) that manifests itself only when the cells are in pellets but not in solution. These data will be compared to theoretical predictions and their significance discussed.*

I. INTRODUCTION

We have shown that during cell death the backscatter from cell ensembles increases by 9-13dB and produces changes both in the normalized frequency spectrum[1, 2] and the backscatter envelope amplitude statistics[3]. However, we have not yet understood the nature of these changes. Variations in ultrasonic backscatter can be attributed to changes in the ultrasonic scatterer size, composition and spatial distribution, all of which may be modified during cell death. Moreover, it is not known what predominantly scatters ultrasound in tissues and tumours making modelling the backscattering process difficult. To better understand the nature of cell backscatter, we investigate the backscatter from cells of different sizes using both 20MHz and 40MHz transducers to examine how cell size influences backscatter. To this end, several models have been proposed to relate normalized spectral slopes to effective scatterer size[4, 5]. For example, Oelze *et al.* measured the power spectra from rat tumors and compared them to theoretical power spectra derived from a 3D spatial autocorrelation function (assuming a Gaussian distribution), allowing the estimation of an average scatterer diameter by approximating the measured power spectrum with a best-fit line. They were able to correlate cellular features from their histology to the ultrasonically derived scatterer diameter. Using the Gaussian form factor model a decrease in spectral slope as a function of scatterer size is predicted. This

is tested in this work for two cell lines of different size and cell to nucleus diameters.

II. METHODS

Separate cultures of Acute Myeloid Leukemia cells (OCI-AML5) and prostate adenocarcinoma cells (PC-3) were grown at a cell density of $3x10^5$cells/ml in α minimum essential medium (GIBCO 11900, Rockville, MD, USA) supplemented with 5% fetal bovine serum (Cansera International, Etobicoke, ON, Canada) at 37±C. Set volumes of cells were placed into a degassed phosphate buffered saline (PBS) solution in a sample holder to form suspensions of various volume concentrations of cells. B-scan images and RF data were acquired from approximately 200 locations from the cell samples (Figure 1). Two broadband transducers were used for imaging: one with a center frequency of 20MHz (8.5mm diameter, f2.3, –6dB bandwidth: 10-30MHz) and the other 40MHz (3mm diameter, f2, –6dB bandwidth: 20-53MHz). The transducers were purchased from VisualSonics Inc. (www.visualsonics.com) and attached to the VS40B ultrasound imager. The VS40B has the ability to select regions of interest from the B-scan images and store the raw radio-frequency (rf) data associated with the region of interest (ROI). The ROI was centered at the transducer focus and was approximately 1 mm in length and several mm in width. The Fourier transform of the ROI was taken using a Hamming apodization function. The power spectrum was obtained by averaging the results from the independent scan lines. This power spectrum was divided by the power spectrum of the echo from a calibration target to obtain the normalized spectra. The perpendicular reflection off a quartz flat located at the focal point of the transducer was used to remove system and transducer transfer functions and provide a common reference for data collected with various transducers[4]. Linear regression analysis was applied to the calibrated spectral amplitudes (converted to dB and labeled dBr).

Following the data acquisition, images of the individual cells were taken with a light microscope to estimate the cell diameter. The concentration of cells was independently measured using a hemocytometer. The cell concentrations varied from 0.0025% by volume (a sparse solution in which single cells were detected ultrasonically) to a cell pellet (created using a swinging bucket centrifuge for 10 minutes at 2000g to form pellets, a compacted aggregate of cells, emulating tissues).

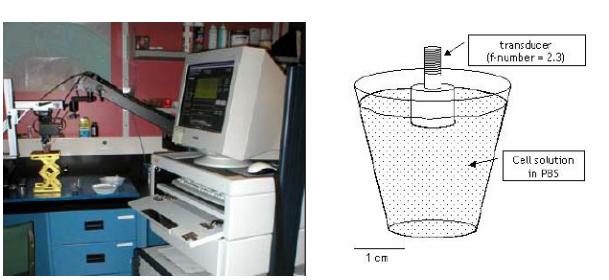

(A) (B)

Figure 1: (A) Photograph of VisualSonics VS-40B instrument imaging cell solutions. (B) Schematic of data acquisition setup. The ultrasonic transducer is immersed in a degassed PBS solution containing AML or PC3 cells or cell pellets.

III. RESULTS

The light microscopy images (Figure 2) reveal the large difference in cell diameter between the two cell lines. Because the PC-3 cells are larger, at the same cell volume concentration the AML suspension has more cells per unit volume than the corresponding suspension of PC-3 cells. This is visible in the B-scan images where at the low concentrations individual cells are resolved (Figure 3). As the cell concentration increases the image forms a speckle pattern as signal contributions are from an increasing number of cells within the resolution volume of the transducer.

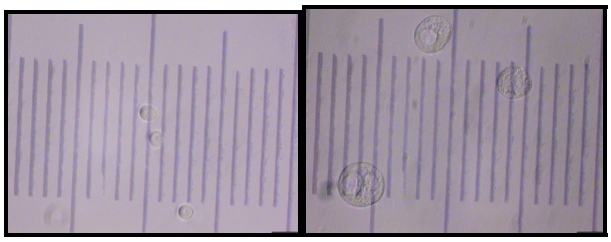

Figure 2: Light microscopy of the AML cells (left) and PC3 cells (right) in PBS solution. Subdivisions in both images are 10μm. The AML cells (diameter 9.8 +/- 1μm) are significantly smaller than the PC3 cells (diameter 25 +/- 6μm).

A comparison of images collected from the prostate and leukemia cells at 0.0025% and 1.6% volumetric concentrations is shown in Figure 4, along with the pellet images. In the single cell (A,D), as well as the pellet images (C,F) the prostate cells are significantly brighter, whereas this is not the case in panels (B,E). At these concentrations the speckle pattern is most likely formed from cells that are distributed *randomly* in the medium.

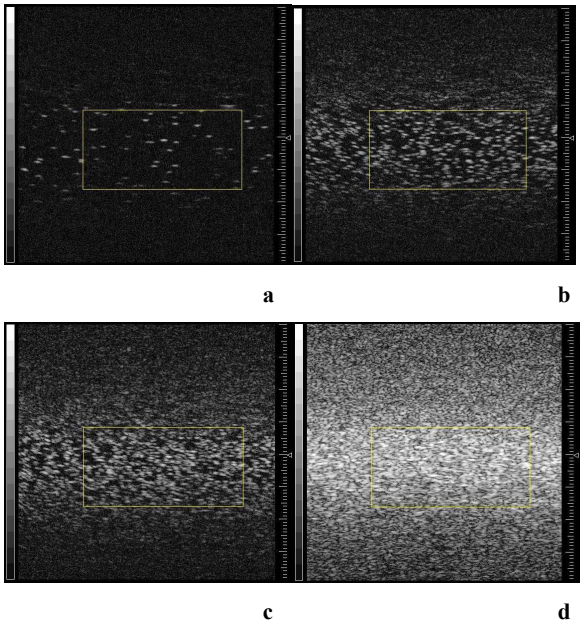

Figure 3: Ultrasonic images (8x8mm) of AML cell solutions acquired using the 20MHz transducer with volumetric cell concentrations of (a) 0.0025% (b) 0.05% (c) 0.1% (d) 0.8%. Images demonstrate the transition from the detection of single cells (a) to the formation of a speckle pattern (d). The bright band in the middle of the images corresponds to the transducer focal zone. Yellow lines in some images correspond to ROIs.

In Figure 5 selected normalized spectroscopic data are presented. The curves were acquired using both the 20MHz and 40MHz transducers, and there is a common region in the power spectra between 20 and 30MHz. The curves generally overlap in this region as expected for normalized power spectra.

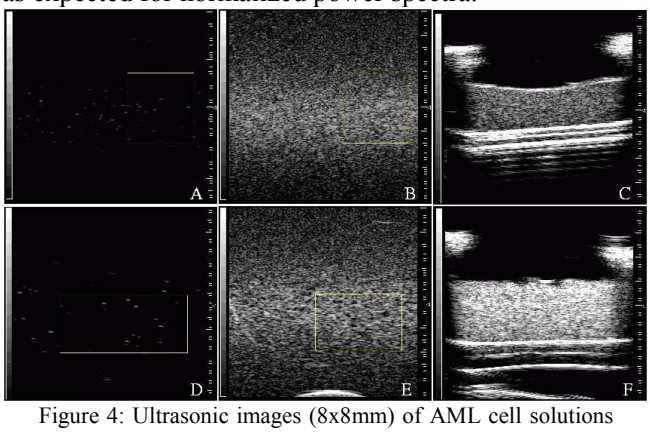

Figure 4: Ultrasonic images (8x8mm) of AML cell solutions (A – 0.0025%, B – 1.6%) and PC3 solutions (D – 0.0025%, E – 1.6%) using the 20MHz transducer. Images of AML (C) and PC3 (F) cell pellets. Bright reflections on the side and bottom represent the pellet container. Note that the gain is same in all images and about 10dB lower than in Figure 3 to avoid excessive pellet image saturation.

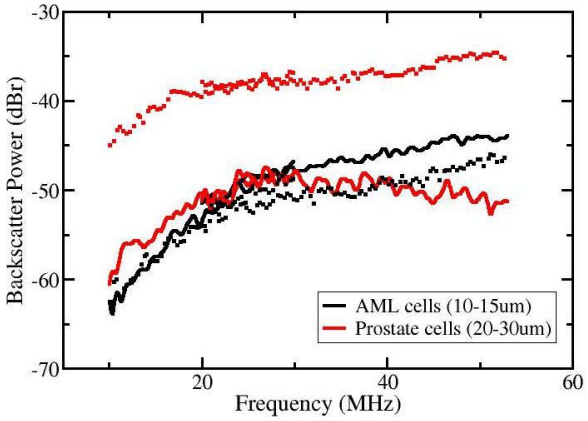

Figure 5: Normalized spectroscopic data, acquired using both 20MHz and 40MHz transducers, of AML cells (black lines) and PC3 cells (red lines). The dashed lines correspond to the pellet data, whereas the solid lines correspond to the 1.6%vol data. Note the change in 40MHz transducer spectral slope from the prostate cells in 1.6%vol solution (red, solid) and the cell pellet (red, dashed). Also notable the similar level of backscatter from AML pellets and a 1.6%vol solution.

IV. DISCUSSION

The cell pellet model is a good starting point for understanding tissue backscatter, as most tissues are composed of cell aggregates. This is especially true of tumor tissues, which is of interest to our group. Moreover, it is our experience that tumors generated by implanting these cells in nude mice generate results similar to those seen in cell pellets.

Figure 3 demonstrates the stages of how, from the detection of single cells, one reaches a speckle pattern by increasing the number of scatterers per resolution volume. Whereas single cells could not be detected outside the focal band, as the number of cells increase the speckle pattern extends outside this band.

It is clear that the cross section for the prostate cells is greater than that of the leukemia cells, as shown in Figure 4A and D. This is expected due to the larger cell size (Figure 2). Similar levels of backscatter can be achieved for the two cells lines at the same volumetric concentration (Figures 4B and E) when the number of cells is sufficient to account for the cross section difference of individual cells. One can assume that the number of cells per resolution volume has reached its maximum when the cells form cell pellets, as they have reached their maximum packing density. It is then interesting to note that for the AML cells, the backscatter power is slightly greater when they form a 1.6%/vol solution than when they form a pellet (Figure 4B and C). This does not hold true for the PC3 cell line (Figure 4E and F).

While it is not clear what may be causing this, the effect may be linked to scatterer randomization. This has been established with red blood cell solutions[6] and theoretically with cells[7]. PC3 cell nuclei occupy a much smaller fraction of the cell than the AML nuclei (for which the nucleus occupies almost the entire cell). Therefore, one may expect greater scatterer randomization for the PC3 pellet if one assumes the nucleus as the scatterer. The spectral data add one more layer of complexity to this argument.

The normalized power spectra in Figure 5 show in a quantitative manner the similarity in backscatter power for the two 1.6% solutions and the large difference for the pellets. At 20MHz, the PC3 cell pellet has an integrated backscatter over 10dB greater than that of the AML pellet, even though there are roughly 8 times more AML cells per resolution volume (assuming a factor of 2 difference in radius). Therefore, it is clear that scattering structures on the order of the size of cells contribute to this signal. This is further substantiated by inspection of the spectral slopes in Figure 5: for the AML cells and at 20MHz, the spectral slopes measured were between 0.7 and 0.83 dBr/MHz, while for the prostate cells between 0.4 and 0.56 dBr/MHz. Using a Gaussian form factor and the (corrected) mathematical derivations published by Lizzi[8], the effective scatterer radii are between 10 to 6.4 μm for the AML cells and 15 and 13 μm for the PC3 cells, in good general agreement with the measured diameters.

A very interesting feature seen in Figure 5 is the change in spectral slope at 40MHz for the PC3 cells: while for *all* the solutions the spectral slope is negative (-0.04 to -0.09 dBr/MHz, resulting in effective scatter radii of 11 to 13 μm), when in pellet form, the spectral slope is positive (0.12 dBr/MHz, for an effective scatterer radius of 9 μm). This is despite the fact that these slopes have not been corrected for attenuation, which would make the pellet spectral slopes even larger (corrections for solutions are not as important as they have negligible attenuation). This strongly suggests that for the PC3 cells, the size of the scattering structure is larger when the cell is in solution compared to when the cell is in pellet form. Moreover, the effective scatterer size would suggest that the nucleus is strongly contributing to backscatter, as we have postulated in previously[1]. Notably, there is no such slope reversal for the AML cells as the nucleus occupies a very large portion of the cell volume. We are now analyzing the amplitude statistics of these signals, which are also expected to reveal information about ultrasonic scatterers.

V. CONCLUSIONS

Cell size is a major determinate of cell backscatter in solutions and cell pellets. Spectral slopes can be used to differentiate backscatter from cells of different sizes, both in solution and in pellets. Finally, slope reversals in the spectral data suggest that the cell nucleus strongly contributes to backscatter when cells are in pellets, but the cytoplasm/solution boundary dominates when cells are in suspension.

ACKNOWLEDGEMENTS

The authors would like to acknowledge the financial support of the Canada Foundation for Innovation, the Whitaker Foundation, the Canadian Institutes of Health Research, the Natural Sciences and Engineering Research Council of Canada, and the Ontario Innovation Trust.

REFERENCES

[1] M. C. Kolios, G. J. Czarnota, M. Lee, J. W. Hunt, and M. D. Sherar, "Ultrasonic spectral parameter characterization of apoptosis," *Ultrasound Med Biol*, vol. 28, pp. 589-97, 2002.

[2] M. C. Kolios, L. Taggart, R. E. Baddour, F. S. Foster, J. W. Hunt, G. J. Czarnota, and M. D. Sherar, "An investigation of backscatter power spectra from cells, cell pellets and microspheres," in *Ultrasonics Symposium, 2003 IEEE*, 2003, pp. 752-757.

[3] A. S. Tunis, G. J. Czarnota, A. Giles, M. D. Sherar, J. W. Hunt, and M. C. Kolios, "Monitoring Structural Changes in Cells with High Frequency Ultrasound Signal Statistics," in *Ultrasound in Medicine & Biology*, vol. submitted for publication, 2004.

[4] F. L. Lizzi, M. Greenebaum, E. J. Feleppa, M. Elbaum, and D. J. Coleman, "Theoretical framework for spectrum analysis in ultrasonic tissue characterization," *J Acoust Soc Am*, vol. 73, pp. 1366-73, 1983.

[5] M. L. Oelze, J. F. Zachary, and W. D. O'Brien, Jr., "Parametric imaging of rat mammary tumors in vivo for the purposes of tissue characterization," *Journal of Ultrasound in Medicine*, vol. 21, pp. 1201-10, 2002.

[6] L. Y. Mo and R. S. Cobbold, "A unified approach to modeling the backscattered Doppler ultrasound from blood," *IEEE Trans Biomed Eng*, vol. 39, pp. 450-61, 1992.

[7] J. W. Hunt, A. E. Worthington, A. Xuan, M. C. Kolios, G. J. Czarnota, and M. D. Sherar, "A model based upon pseudo regular spacing of cells combined with the randomisation of the nuclei can explain the significant changes in high-frequency ultrasound signals during apoptosis," *Ultrasound Med Biol*, vol. 28, pp. 217-26, 2002.

[8] F. L. Lizzi, M. Astor, A. Kalisz, T. Liu, D. J. Coleman, R. H. Silverman, R. Ursea, and M. J. Rondeau, "Ultrasonic spectrum analysis for assays of different scatterer morphologies: theory and very-high frequency clinical results," presented at 1996 IEEE Ultrasonics Symposium, 1996.

*Corresponding author: M.C. Kolios, e-mail: mkolios@ryerson.ca